Time-Resolved Hole-Burning Study on Myoglobin: Fluctuation of Restricted Water within Distal Pocket

Yutaka Shibata,*† Haruto Ishikawa,‡ Satoshi Takahashi,*‡ and Isao Morishima‡

*Precursory Research for Embryonic Science and Technology (PRESTO), Japan Science and Technology Corporation, and †Institute for Laser Technology, Hyogo 661-0974, and ‡Department of Molecular Engineering, Graduate School of Engineering, Kyoto University, Kyoto 606-8501, Japan

ABSTRACT We have studied the equilibrium fluctuation dynamics of Zn-substituted myoglobin and its His64→Leu (H64L) mutant in the pH range from 5 to 9 by using time-resolved transient-hole-burning (TRTHB) spectroscopy. In the H64L mutant, we have observed a largely reduced width of the absorption spectrum and only a slight temporal shift of the hole-burning spectrum. These observations both reflect the suppressed conformational fluctuation in the mutant. On the other hand, the pH-dependent change in the absorption spectrum could not be solely explained by the change in the protonation state of His64 induced by the pH change. These results suggest that although the fluctuation dynamics observed by the TRTHB experiment of the native sample mainly reflects the conformational motion around His64, the interconversion process of His64 between its protonated and unprotonated states has a minor contribution. Instead, we have proposed a tentative interpretation that the motion of the water molecule around His64 is the main source of the observed dynamics in the TRTHB technique.

INTRODUCTION

Myoglobin (Mb), which is an O_2-storage protein, has been one of the most simple and important model systems for investigating the relation between function and dynamics of protein (Austin et al., 1975; Ansari et al., 1985; Frauenfelder et al., 1991; Young et al., 1991; Jackson et al., 1994). Intensive studies on this protein for the past 30 years have revealed the crucial role of conformational fluctuation for the entrance and exit of a small ligand molecule (Barboy and Feitelson, 1989; Elber and Karplus, 1990; Carlson et al., 1996; Tian et al., 1996). Fluctuation of the distal-pocket residues in deoxy-Mb may be coupled to motions of water molecules within the pocket, which has been indicated by mutant studies to play an important role in determining the association rate of a ligand molecule (Carver et al., 1990; Quillin et al., 1993; Uchida et al., 1997). Conformational fluctuation may have a general role in controlling the entrance, exit, and diffusion processes of small molecules within a protein matrix. It has been also suggested that the internal water molecules within the protein matrix play an important role in maintaining the conformational flexibility of protein (Sastry and Agmon, 1997).

Recently, we have developed a novel method of time-resolved transient-hole-burning (TRTHB) spectroscopy, which provides us with an opportunity to make time-domain observation of conformational fluctuation dynamics of a protein over a wide time range from nanosecond to millisecond (Shibata et al., 1997, 1998, 1999). The principle of the TRTHB method is summarized as follows (Kinoshita, 1989; Shibata et al., 1998, 1999). We consider an absorption spectrum of a solution of chromoprotein with fluctuating conformation, which perturbs the resonance energy of the contained chromophore. Each single chromophore has different resonance energy depending on its surrounding environment. The temporal fluctuation of protein conformation induces the fluctuation of the environment of the chromophore and then induces the temporal fluctuation of its resonance energy. By detecting this spectral diffusion phenomenon, one can make a time-domain observation of the conformational fluctuation of a protein matrix. In the TRTHB method, this is done by detecting the temporal change in the transient-hole-burning (THB) spectrum burned by an irradiation of a laser pulse. The irradiation of a spectrally sharp laser pulse selectively excites the chromophores that are resonant with the laser wavelength. Until the excited molecules relax to the ground state, a hole is observed around the laser frequency in the absorption spectrum. This THB spectrum varies with time because of spectral diffusion. Hence, the conformational fluctuation of a protein can be detected by observing this temporal variation of the THB spectrum until the excited molecules relax. We have employed myoglobin samples in which the intact heme is substituted by Zn-protoporphyrin IX (Zn-PP). In this case, accumulating the excited molecules in the long-lived triplet state results in hole burning. Consequently, the lifetime of the hole becomes as long as the phosphorescence lifetime, typically in the millisecond region. One can therefore make a time-domain observation of the conformational fluctuation over the nanosecond to millisecond time range.

In previous studies using the TRTHB technique, we have succeeded in deriving novel aspects of conformational dynamics of Zn-substituted Mb (Zn-Mb). These investigations

Received for publication 14 August 2000 and in final form 16 November 2000.

Address reprint requests to Dr. Yutaka Shibata, Institute for Laser Technology, c/o Kansai Electric Power Co., 3–11-20 Nakoji, Amagasaki, Hyogo 661-0974, Japan. Tel.: 81-66492-7613; Fax: 81-66492-5641; E-mail: yshibata@ile.osaka-u.ac.jp.

0006-3495/01/02/1013/11 $2.00

have revealed a highly non-exponential time dependence of fluctuation dynamics of Mb. Observed temporal change is well described by a stretched-exponential function ($\exp[-(t_d/\tau_c)^{\beta}]$), with $\beta = 0.26$ (Shibata et al., 1998, 1999). A value of β of 0.26 is a conspicuously small value as compared with those for typical glass-forming liquids, probably reflecting the high structural complexity and hierarchy of Mb. Rather slow dynamics ranging up to the microsecond time region even at room temperature also implies the liquid-like nature of the protein fluctuation. Furthermore, our study has observed a strong correlation between solvent viscosity and the time scale τ_c of the fluctuation. τ_c has been found to obey a linear relation to solvent viscosity, without any apparent temperature dependence (Shibata et al., 1999).

Although these studies have revealed novel dynamical aspects of Mb, so far it is not clear what is the structural origin of the observed temporal variation of the THB spectrum. To connect the observed dynamical properties with functional aspects of Mb, a structural model for what is the origin of the observed dynamics is indispensable. The focus of the present study is to determine what is the structural origin of the observed process. To achieve this purpose, here we study the effect of site-directed mutation and also that of pH change on the TRTHB experiment. The experimental results are analyzed based on the known structural data of intact Mb and Zn-Mb obtained from x-ray diffraction studies (Quillin et al., 1993; Yang and Phillips, 1996; Vojtvěchovský et al., 1999) and spectroscopic studies (Feitelson and Spiro, 1986; Müller et al., 1999). Zn-Mb used in the TRTHB experiment has been clarified to adopt the deoxy-Mb-like structure by Raman-scattering investigation (Feitelson and Spiro, 1986). Our previous studies have also shown almost the identical secondary structure between Zn-Mb and intact Mb (Shibata et al., 1998). Although there is no direct measurement of the tertiary structure of Zn-Mb so far, we consider based on the above observation that Zn-Mb has almost the same conformation as that of deoxy-Mb.

To date, x-ray diffraction studies on Mb have provided information about its structure and dynamics. Yang and Phillips (1996) have determined the crystal structures of Mb at various pH values and in various ligation states. Their study has clarified the flexibility of the distal histidine (His64) residue. In low pH condition, His64 is protonated and its imidazole ring tends to point toward the solvent side. This tendency is especially obvious in the carbonmonoxy state and is also valid in the deoxy state. Recently, Vojtvěchovský et al. (1999) have determined the crystal structure of Mb at near-atomic resolution. This study has suggested that His64 assumes two slightly different conformations with equal occupancy in deoxy-Mb at neutral pH. These two conformers may correspond to those observed by Yang and Phillips at low- and high-pH conditions. These investigations have suggested that, in deoxy-Mb at room temperature the distal His fluctuates between the two distinct conformations.

Recently, Müller et al. (1999) have revisited the pH dependence of the CO-stretching band of MbCO and established the structural model for the *A* substates (Alben et al., 1982; Frauenfelder et al., 1991). Based on site-directed mutagenesis and the singular-value decomposition analysis, they have shown that the pH-dependent variation of the band profile can be interpreted as coming from the pH-dependent change in the protonation states of His64 and His97. They have shown that the pH-dependent protonations of these residues obey the simple uncoupled Henderson-Hasselbach relation. A model considering three protonation states for these residues can give a quantitative explanation of the pH dependence of the CO-stretching band. The three states include that in which both residues are unprotonated at high pH, that in which these residues are in equilibrium between protonated and unprotonated states at intermediate pH, and that in which both residues are protonated at low pH.

X-ray diffraction and spectroscopic investigations described above provide us with a hint to clarify the structural origin of the fluctuation dynamics observed in the TRTHB method. A rather mobile character of His64 revealed by these studies helps us consider the motion of His64 as a plausible candidate for the origin of the fluctuation process observed by TRTHB. Indeed, the polar His64 and the water molecule hydrogen-bonded to it seem likely to strongly perturb the electronic state of porphyrin. In the present paper, therefore, we focus our interest on the relation between the conformational motion around His64 and the fluctuation process observed by the TRTHB technique. We study the effect of site-directed mutation, His64→Leu (H64L), and also variation of pH on the fluctuation dynamics observed by the TRTHB technique. X-ray diffraction study of the H64L mutant has clarified that the replaced Leu residue points into the heme pocket. It has been also revealed that the water molecule hydrogen-bonded to His64 in the native protein is excluded from the heme pocket in the mutant due to the hydrophobic nature of the Leu residue (Quillin et al., 1993). As indicated above, variation of pH causes a conformational change in His64. To study the effect of this conformational alteration of His64 by changing pH will help to clarify what is the structural origin of the observed process in more detail.

MATERIALS AND METHODS

Sample preparation

As in the case of the previous TRTHB studies, in the present investigation we have employed horse Mb (hsMb) as the native-type sample. hsMb was purchased from Sigma Chemical Co. (St. Louis, MO) and used without further purification. Mutant and wild-type human Mb (hmMb) were prepared as described previously (Varadarajan et al., 1985; Uchida et al., 1997). We have done a control TRTHB experiment for the wild-type Zn-hmMb and confirmed that there is no obvious difference in the fluctuation dynamics between Zn-hsMb and Zn-hmMb. Thus, we conclude

here that the difference of experimental results between Zn-hmMb-H64L and Zn-hsMb mainly comes from the effect of site-directed mutation.

The substitution of Zn-protoporphyrin IX (Zn-PP) for the heme in intact Mb for all Mb samples has been done by the same procedure as that in the previous studies (Kurita et al., 1990). For low-temperature experiments, Zn-Mb solution in 100 mM phosphate buffer (pH 6.0) was mixed with a threefold volume of glycerol (Zn-Mb/W:3G) to maintain its transparency. The protein concentration of this solution was ~0.3 mM. For measurements of the pH dependence at room temperature (296 ± 0.5 K), the pH of sample solutions was controlled according to Müller et al. (1999). Namely, Zn-hsMb solution was mixed with a threefold volume of 400 mM buffer with desired pH, resulting in again ~0.3 mM protein solution in ~300 mM buffer. The pH of the prepared solutions was determined by using a semiconductor-based pH meter (pHBOY-P2, Shindengen, Tokyo, Japan) after mixing. Acetic acid/sodium acetate buffer, phosphate buffer, and glycine/NaOH buffer were used for pH regions below 5, between 5 and 8, and above 8, respectively.

Spectroscopic methods

The experimental method is basically the same as that reported in the previous papers (Shibata et al., 1997, 1998, 1999). The wavelength of the burning laser is of practical importance. To observe a large temporal shift of the THB spectrum, burning should be made in the red edge of the absorption spectrum. In the present study, the burning wavelength was carefully chosen in the red-edge region of the absorption spectrum so that the optical density at the burning wavelength was ~25% of the absorption maximum. Because the profile of the absorption spectrum is temperature dependent, we adjusted the burning wavelength at each temperature. Furthermore, to obtain the THB spectrum free from the rotational-relaxation effect of a protein, we observed the THB spectrum in the magic-angle configuration in which the angle θ between the polarizations of the probe and burning beams satisfies the relation $\sin^2\theta = 2\cos^2\theta$. Some minor changes in experimental instruments have been made as follows.

For cryogenic experiments, the sample solution was contained in a handmade copper cell having glass windows and cooled with a closed-type refrigerator (model V202C5L, Daikin Industries, Osaka, Japan). Its temperature was controlled within ±0.1 K accuracy. For room-temperature aqueous-solution experiments, the sample solution was sealed within a glass cell without any temperature-control equipment. The optical-path length was 2 mm for both cryogenic and room-temperature experiments.

The burning was made by using a dye laser (FL3002E, Lambda Physik, Göttingen, Germany using rhodamine 6G dye) with a pulse duration of ~7 ns, pumped by a frequency-tripled and Q-switched Nd:YAG laser (LAB-130, Spectra Physics, Mountain View, CA). For the probe-light source, we used a nanosecond pulse lamp (Xenon, model-437B, Weburn, MA). Its pulse duration and time jitter were ~10 ns and ±5 ns, respectively, which limited the temporal resolution of our measurement to be ~20 ns. A small fraction of collimated probe light was reflected by a wedged glass plate, focused into one input of the *y*-blanched optical fiber and used as a spectral reference. The main part of the probe light was transmitted through the sample and then focused into the other input of the *y*-blanched fiber. The output of the optical fiber was guided into a polychromator (model 320i, Acton Research, Acton, MA), and the spectra of both the sample and the reference were detected by an air-cooled CCD-camera system (model TEA/CCD-1100PF/UV, Princeton Instruments, Trenton, NJ). The THB spectrum at time t_d after the burning was obtained as

$$H(\nu, t_d) \equiv A'(\nu, t_d) - A(\nu) = \log_{10}\left[\left(\frac{I^{sig}(\nu, t_d) - I^{sig}_{laser}(\nu)}{I^{sig}_0(\nu)}\right)\Big/\left(\frac{I^{ref}(\nu, t_d) - I^{ref}_{laser}(\nu)}{I^{ref}_0(\nu)}\right)\right]. \quad (1)$$

Here, $A(\nu)$ is the ordinary absorption spectrum before the burning, and $A'(\nu, t_d)$ is the absorption spectrum at t_d after the burning. $I^{sig/ref}$, $I^{sig/ref}_{laser}$, and $I^{sig/ref}_0$ are the signal/reference light spectrum under the irradiation of both burning and probe pulses, under the burning pulse, and under the probe pulse, respectively.

THEORETICAL BACKGROUND

Here we review the theoretical background relevant to the present study. The absorption spectrum of a chromoprotein solution is given as a convolution of the absorption profile of a single chromoprotein molecule, $a(\nu)$, and inhomogeneous distribution function, $G(\nu_0)$, as

$$A(\nu) = \int a(\nu - \nu_0)G(\nu_0)d\nu_0. \quad (2)$$

Here, ν_0 is the frequency of zero-phonon line, which corresponds to the purely electronic transition without excitation and de-excitation of vibrational modes. ν_0 is called site energy, and $a(\nu)$ is called single-site absorption profile. Here, we assumed that each chromophore has the same single-site absorption profile but with a different site energy. Inhomogeneous distribution arises from the disorder of the environment around the chromophore, which raises or lowers the site energy ν_0 of each molecule randomly. In the case of a protein, the origin of the disorder is conformational substates (CSs) (Austin et al., 1975; Frauenfelder et al., 1979, 1991). Transitions among CSs induce a temporal fluctuation of ν_0 of each molecule, and this phenomenon is called spectral diffusion. The widths of $a(\nu)$ and $G(\nu_0)$ are called homogeneous and inhomogeneous broadening, respectively. It has been demonstrated that the spectral profiles of both $a(\nu)$ and $G(\nu_0)$ can be determined experimentally by using the fluorescence-line-narrowing technique at cryogenic temperatures (Ahn et al., 1995).

If the profiles of both $a(\nu)$ and $G(\nu_0)$ can be approximated by Gaussian shape, the second power of the absorption width is roughly equal to the sum of the second powers of the inhomogeneous broadening and the homogeneous broadening. Above the glass-like transition point, the amplitude of spectral diffusion decreases with lowering temperature. Thus, inhomogeneous broadening decreases with lowering temperature. Homogeneous broadening originates dominantly from the interaction between the chromophore and the low-frequency vibrational modes of the protein (Ahn et al., 1995; Shibata et al., 1996). Then, homogeneous broadening also decreases with lowering temperature because of the reduction of the thermal population of the low-frequency modes. Above the glass-like transition, hence, the temperature dependence of the absorption spectrum is attributed to those of both inhomogeneous and homogeneous broadening. Below the glass-like transition point, on the other hand, the transitions among CSs are frozen, and then inhomogeneous distribution is no longer

temperature dependent. In this case, the temperature dependence of the absorption profile is attributed only to that of the single-site spectrum.

In the TRTHB method, the spectral diffusion process is observed by using the site-selective excitation. By introducing a conditional probability $D(\nu_1, t; \nu_0)$ defined as the fraction of the chromophores having the site energy ν_1 at time t when they initially have the site energy ν_0, the THB spectrum $H(\nu, t_d; \nu_L)$ at time t_d after the burning is expressed as

$$H(\nu, t_d; \nu_L) \propto -\iint a(\nu - \nu_1)D(\nu_1, t_d; \nu_0)a(\nu_L - \nu_0)G(\nu_0)d\nu_1 d\nu_0. \quad (3)$$

Here, ν_L is the frequency of the burning light. It should be stressed that both the temporal variation of the THB spectrum and the inhomogeneous broadening originate from the same fluctuation process, that is, the transition among CSs. Thus, the aim of the present study to clarify the origin of the temporal variation of the THB spectrum is, in other words, to clarify the origin of the inhomogeneous broadening.

RESULTS AND ANALYSIS

Effect of pH change and mutation on absorption spectrum

Fig. 1 *a* shows the pH dependence of the absorption spectrum of Zn-hsMb in a buffered-water solution. Fig. 1 *b* is the same as Fig. 1 *a*, but in this panel the peak heights of the spectra are normalized to unity for comparison and the absorption spectrum of Zn-hmMb-H64L in buffered-water solution at neutral pH is also shown. Fig. 1 clearly shows the spectral shift of the absorption spectrum of Zn-hsMb toward the long-wavelength side with raising pH. It is conspicuous that the absorption spectrum for Zn-hmMb-H64L is located at a much longer wavelength than that for the native sample. Furthermore, it has a much sharper width. This conspicuous effect of the substitution of His64 on the absorption profile indicates that the position-64 residue indeed has a strong influence on the electronic state of Zn-PP. Because of the band sharpening, the side band located ~12 nm shorter wavelength than the main band is more clearly resolved for Zn-hmMb-H64L/W:3G than for the native sample. We have indicated previously by studying the polarization dependence of the THB spectrum that this side band originates from the *x*-*y* splitting of the Q band (Shibata and Kushida, 1998). In the following, we give attention only to the properties of the main band, which more directly reflects the fluctuation dynamics of the protein matrix.

To estimate the peak position and the spectral width of the absorption profile, we numerically calculated the first

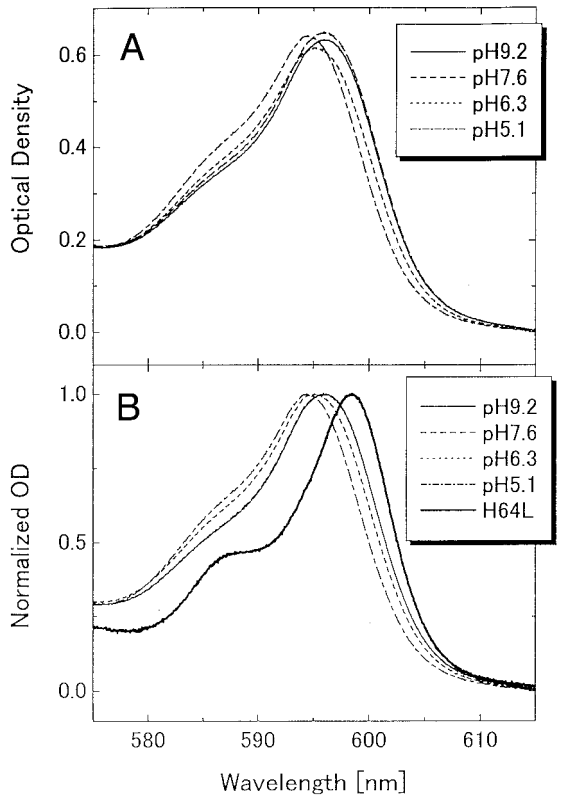

FIGURE 1 (*a*) Q-band absorption spectrum of Zn-hsMb in aqueous solutions at various pH values. Protein concentration is same for every sample. (*b*) Normalized Q-band absorption spectrum of Zn-hsMb at various pH values and that of Zn-hmMb-H64L at neutral pH (*thick line*). The lines for Zn-hsMb at pH 7.6 and pH 9.2 almost completely overlap and cannot be distinguished from each other.

moment M_1 and the dispersion σ^2 of the absorption spectra as

$$M_{1abs} \equiv \frac{\int_{\nu_1}^{\nu_2} \nu A(\nu)d\nu}{\int_{\nu_1}^{\nu_2} A(\nu)d\nu} \quad (4)$$

$$\sigma_{abs}^2 \equiv \frac{\int_{\nu_1}^{\nu_2} (\nu - M_{1abs})^2 A(\nu)d\nu}{\int_{\nu_1}^{\nu_2} A(\nu)d\nu}. \quad (5)$$

Here, integration was carried out in the energy unit cm^{-1} within the spectral region between ν_1 and ν_2. We selected the energy positions where the height of the spectrum is 20% in the low-energy side and 80% in the high-energy side of its maximum as the low-energy (ν_1) and high-energy (ν_2) limits of the calculation, respectively. The subscript abs indicates that these values are calculated for the absorption spectrum. It should be noted that σ approximates half of the spectral width.

Fig. 2, *a* and *b*, show the pH dependence of M_{1abs} and σ_{abs} for Zn-hsMb, respectively. It is clear that the pH-dependent shift of the absorption spectrum occurs mainly in the pH region from 5 to 7. On the other hand, the dispersion of the absorption spectrum within this pH region is slightly

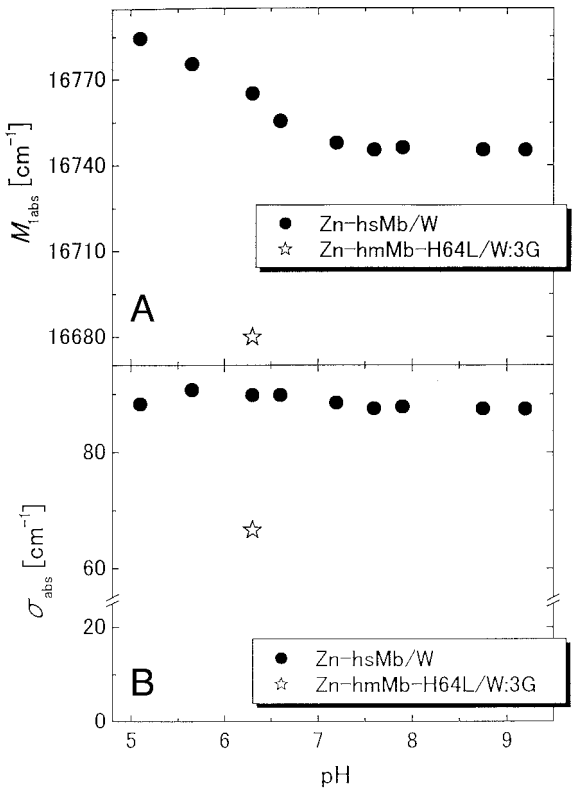

FIGURE 2 pH dependence of M_{1abs} (*a*) and σ_{abs} (*b*) calculated for the Q-band absorption spectrum of Zn-hsMb in aqueous solution (●) and that of the H64L-mutant in aqueous solution (☆).

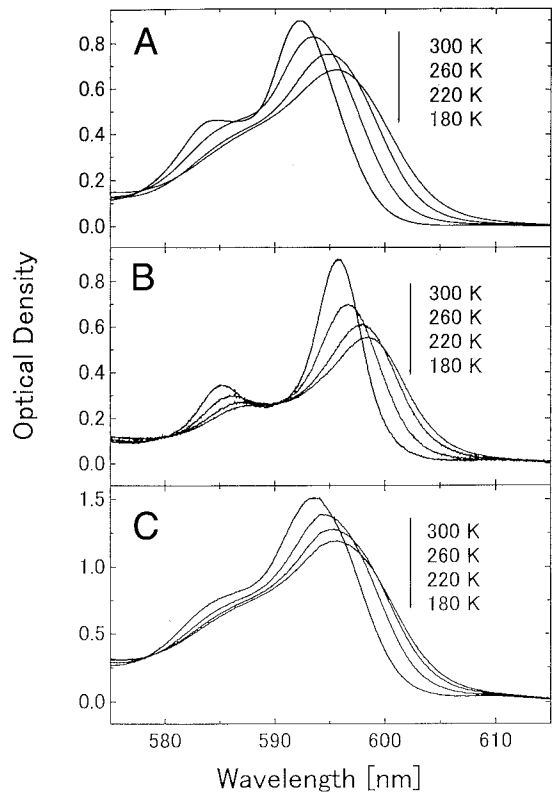

FIGURE 3 Temperature dependence of the Q-band absorption spectrum of Zn-hsMb/W:3G (*a*), Zn-hmMb-H64L/W:3G (*b*), and Zn-hmMb/W:3G (*c*).

larger as compared with that outside this pH region. Müller et al. (1999) have shown that the change in the CO-stretching-band profile of sperm whale MbCO (swMbCO) with varying pH mainly takes place also in this 5–7 pH region. They have reasonably interpreted that the pH-dependent spectral variation of the CO-stretching band is caused by the change in the protonation states in His64 and His97 taking place in this pH region. The estimated pK values are 4.53 and 5.91 for His64 and His97, respectively. The fact that the pH-dependent variation of both the Q-band absorption spectrum of Zn-hsMb and the CO-stretching band of swMbCO occurs in the same pH region seems to indicate that the present pH-dependent shift of the absorption spectrum is also induced by the conformational change in His64 upon pH change. As discussed in detail later, however, only a slight broadening of the absorption spectrum in the pH region of 5–7 contradicts at a quantitative level this simple interpretation.

Temperature dependence of absorption spectrum

Fig. 3 compares the temperature dependence of the absorption profile among Zn-hsMb, Zn-hmMb, and Zn-hmMb-H64L in water-glycerol (1/3, v/v) mixtures. All samples show substantial spectral sharpening and shifts toward the short-wavelength side with lowering temperature. Temperature dependencies of the absorption profiles for Zn-hsMb and Zn-hmMb are similar, except for a slightly stronger temperature-dependent shift for Zn-hsMb than that for Zn-hmMb. Although it is not clear, there is an additional difference between the absorption profiles of the H64L-mutant and the native samples. The spectral shape of the main band for the H64L sample is well fitted to a single Gaussian profile (not shown), although it is rather asymmetric and no longer fitted to a single Gaussian form for the native samples, as shown more clearly in the low-temperature spectra in Fig. 3. The asymmetric features of the absorption profiles for the native samples may be attributed to their asymmetric inhomogeneous distributions. Here, we interpret it as implying multiple conformational states for the native samples.

Fig. 4, *a* and *b*, respectively, shows the temperature dependence of M_{1abs} and σ_{abs} for Zn-hsMb (closed circles), Zn-hmMb (open triangles), and Zn-hmMb-H64L (open stars). Zn-hmMb has a slightly broader absorption width than Zn-hsMb. Comparison of σ_{abs} between Zn-hmMb and Zn-hmMb-H64L reveals that the H64L mutation results in an ~30 cm^{-1} reduction of the dispersion of the absorption. In the previous paper, we have determined the inhomogeneous-distribution profile of Zn-hsMb/W:3G at various temperatures (Shibata et al., 1996). The method to determine the $G(\nu_0)$ profile is as follows. The single-site absorp-

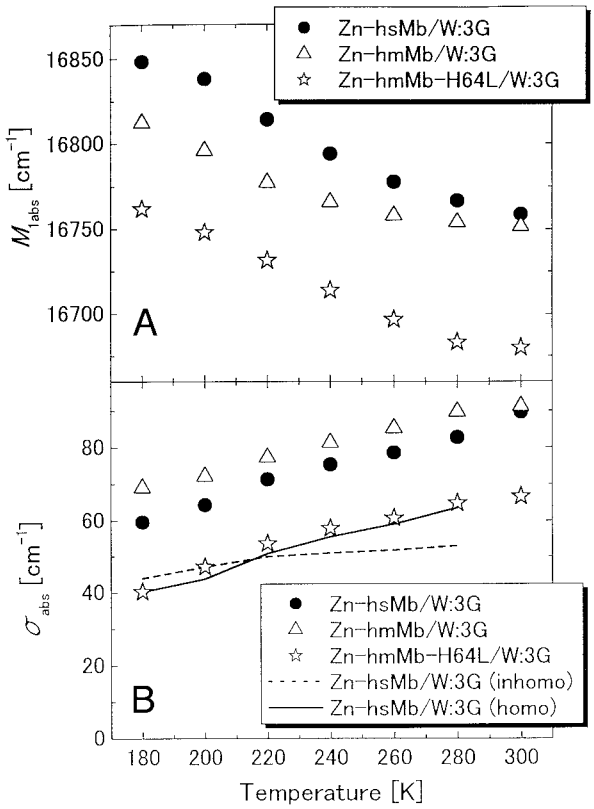

FIGURE 4 Temperature dependence of M_{1abs} (*a*) and σ_{abs} (*b*) calculated for the Q-band absorption spectra of Zn-hsMb/W:3G (●), Zn-hmMb/W:3G (△), and Zn-hmMb-H64L/W:3G (☆). The dashed line and solid line in *b* show, respectively, the temperature dependence of dispersions of the inhomogeneous distribution and the single-site absorption profile of Zn-hsMb/W:3G, which have been determined from simulation (see text).

tion profile at a given temperature can be numerically simulated by using the experimentally obtained information concerning the density of states of the low-frequency modes of Zn-Mb (Ahn et al., 1995; Shibata et al., 1996; Shibata, 1997). By using this simulated single-site absorption profile, the experimentally obtained absorption profile, and numerical deconvolution, the inhomogeneous-distribution profile at a given temperature is determined. The dashed line in Fig. 4 *b* shows σ_{inhomo}, the dispersion of the determined inhomogeneous distribution. The solid line is a rough estimation of σ_{homo}, the dispersion of the single-site absorption calculated as $\sqrt{\sigma_{abs}^2 - \sigma_{inhomo}^2}$. Here, the solid line does not show the temperature dependence of the dispersions of the simulated single-site absorption profiles. This is because they have rather structured shapes and are not appropriate for the numerical integration to estimate their dispersion.

It is obvious in Fig. 4 *b* that homogeneous and inhomogeneous broadening make comparative contributions to the absorption width in the native sample. Conspicuously, σ_{abs} for the H64L sample is almost same as σ_{homo}. If the homogeneous broadening is the same between the native and the H64L samples, this coincidence suggests that the inhomogeneous broadening of the H64L sample is very small. As shown later, however, inhomogeneous broadening of the mutant sample is not zero. Probably the homogeneous broadening of the mutant sample is slightly smaller than the native sample. It is also possible that σ_{homo} is overestimated in the above described procedure because the assumption of Gaussian profiles for $G(\nu_0)$ and $a(\nu)$ is not valid. Anyway, we can say here that inhomogeneous broadening is substantially reduced in the H64L mutant.

Effect of mutation on temporal behavior of THB spectrum

Comparison of the THB spectrum between the native sample and the mutant sample may reveal which is the main source of the reduction of the absorption width for the mutant sample, homogeneous or inhomogeneous broadening. If the sharpening of the homogeneous broadening is the main reason, the THB spectrum should become considerably sharper for the mutant sample. It is also expected in this case that the shift between the THB and the absorption spectra in the mutant sample remains comparative to that of the native sample. Fig. 5 compares the temporal variation of the THB spectrum at 180 K and 240 K between Zn-hsMb/W:3G and Zn-hmMb-H64L/W:3G. The depths of the THB spectra are normalized to unity. The dashed lines in Fig. 5 are the absorption spectra at the respective temperatures whose peak heights are also normalized. It is obvious in Fig. 5 that the hole widths do not differ critically between Zn-hsMb and Zn-hmMb-H64L. The THB spectrum just after the burning for the native sample is shifted toward the long-wavelength side where the burning was made because of the site-selected excitation, whereas only a slight shift is observed in the case of the H64L mutant. These observations provide clear evidence that the reduced absorption width for the H64L mutant mainly comes from the reduction of the inhomogeneous broadening, not from that of the homogeneous broadening. The observation of a slight shift of the THB spectrum from the absorption spectrum, on the other hand, indicates that the inhomogeneous broadening is indeed non-zero in the H64L mutant.

The temporal variations of the THB spectra at 240 K are quite different between these two samples. The THB spectrum for Zn-hsMb shows a large temporal shift toward the absorption maximum and at last results in almost the same spectral shape as that of the absorption spectrum. Contrary to this, the THB spectrum for Zn-hmMb-H64L shifts only slightly with time at 240 K. It has almost the same profile as that of the absorption spectrum even just after the burning. This again confirms a reduced inhomogeneous broadening for the H64L mutant.

To characterize the temporal shift of the THB spectrum, we introduce as in the previous papers (Shibata et al., 1998, 1999) a function $c(t_d) \equiv M_{1THB}(t_d) - M_{1abs}$, that is, the difference of the first moment between the absorption and

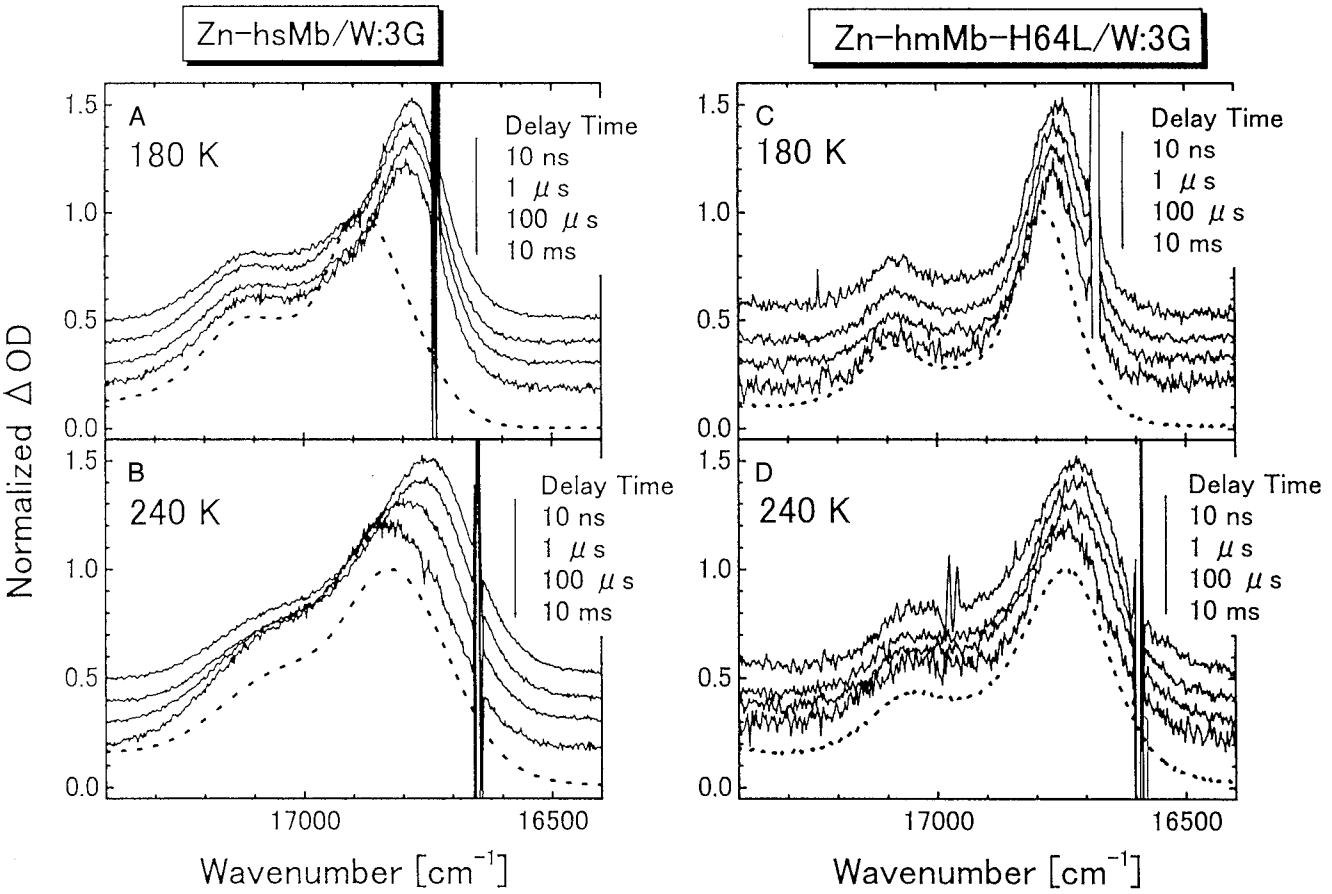

FIGURE 5 Time-evolution of the normalized THB spectra of Zn-hsMb/W:3G at 180 K (*a*) and 240 K (*b*) and those of Zn-hmMb-H64L/W:3G at 180 K (*c*) and 240 K (*d*). The spectra are offset vertically to avoid overlap. The dashed lines denote the normalized absorption spectra.

THB spectra. M_1 is the first moment of the spectrum as defined in Eq. 4, and the subscripts THB/abs indicate the values as calculated for the THB/absorption spectra. The function $c(t_d)$ is expected to tend to 0 in the time region well beyond the conformational-fluctuation time scale (Shibata et al., 1998, 1999). Here, we again selected the spectral positions where the height of the spectrum is 20% and 80% of its maximum as the low- and high-energy limits of the integration, respectively, to exclude the side band in the high-energy side from the calculation. Furthermore, we eliminated the distortions due to the laser scattering in the observed THB spectra by approximating the spectra around the laser wavelength with appropriate quadratic functions.

Fig. 6 compares the temporal evolutions of $c(t_d)$ between Zn-hsMb/W:3G (Fig. 6 *a*) and Zn-hmMb-H64L/W:3G (Fig. 6 *b*). The $c(t_d)$ for Zn-hmMb-H64L/W:3G shows only small temporal shifts reflecting its sharp inhomogeneous broadening. The $c(t_d)$ for Zn-hmMb/W:3G, not shown here, shows a similar temporal variation with a similar temperature dependence to that of Zn-hsMb/W:3G, indicating that the conspicuous tendency of $c(t_d)$ for the H64L-mutant sample is a result of the mutation. The solid lines in Fig. 6 *a* are the fitting curves to the stretched-exponential function as discussed in the previous papers (Shibata et al., 1998, 1999). The slowing down of the time scale of the temporal shift of $c(t_d)$ for the native samples has been interpreted as reflecting the glass-like transition of the protein matrix. In the case of the H64L sample, the absolute value of $c(t_d)$ is much smaller than that of the native sample, indicating the reduced inhomogeneous broadening. Despite its small amplitude and severe scattering of the data points, however, we can recognize temporal shifts of $c(t_d)$ for the H64L sample in the 220–240 K temperature region. The amplitude of the shift amounts to $\sim$20 cm^{-1} at 240 K, which is $\sim$40 cm^{-1} smaller than that observed for the native sample. The time scale of the temporal shift of $c(t_d)$ for the H64L mutant seems almost the same as that for the native sample. It becomes slower with lowering temperature, probably due to the glass-like transition.

Effect of pH change on temporal behavior of THB spectrum

The His64 residue strongly influences the absorption spectrum of Zn-Mb, as shown above. Therefore, it is expected

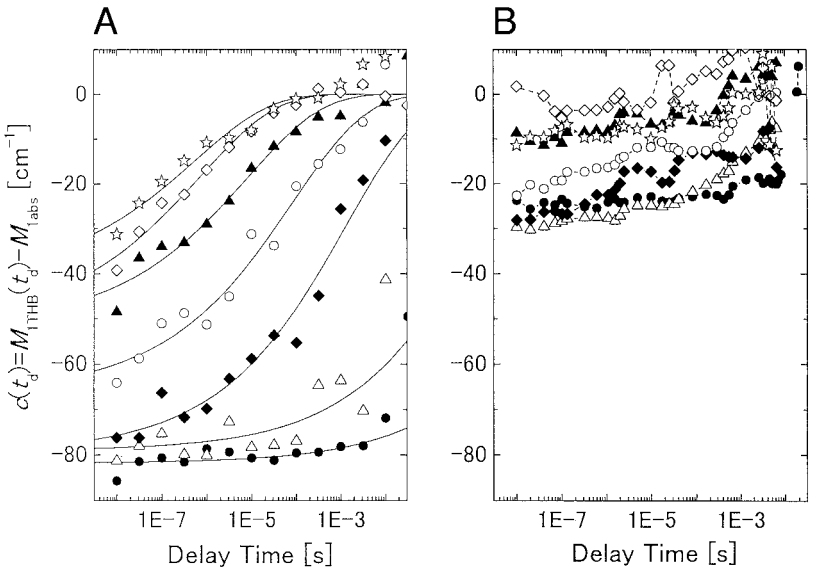

FIGURE 6 Time evolution of $c(t_d)$ for Zn-hsMb/W:3G (*a*) and Zn-hmMb-H64L/W:3G (*b*) at 180 K (●), 200 K (△), 220 K (◆), 240 K (○), 260 K (▲), 280 K (◇), and 300 K (☆). The solid lines in *a* are the fitting curves to the stretched exponential form. The data points at the same temperature in *b* are linked to each other by dashed lines to guides the eye.

that its conformational and protonation-state alterations with varying pH affect considerably the dynamics observed by the TRTHB technique. The experimental results are, however, contrary to this expectation. Fig. 7 shows $c(t_d)$ for Zn-hsMb in aqueous solutions with various pH. The $c(t_d)$ for every pH value shows almost the identical temporal behavior. Its temporal shift lasts up to ~1 μs, and the amplitude of the shift is ~15 cm^{-1} for every sample. The time scale of the temporal shift of $c(t_d)$ becomes somewhat faster than the case of the water-glycerol mixture samples, in which the temporal shift of $c(t_d)$ lasts up to a few tens of microseconds even at room temperature. We can conclude here, despite serious scattering of the data points in Fig. 7, that there seems no evident reduction of the temporal-shift amplitude of $c(t_d)$ by raising pH from 6 to 9. The conformational fluctuation dynamics of the native sample does not seem to depend dramatically on the protonation state of His64.

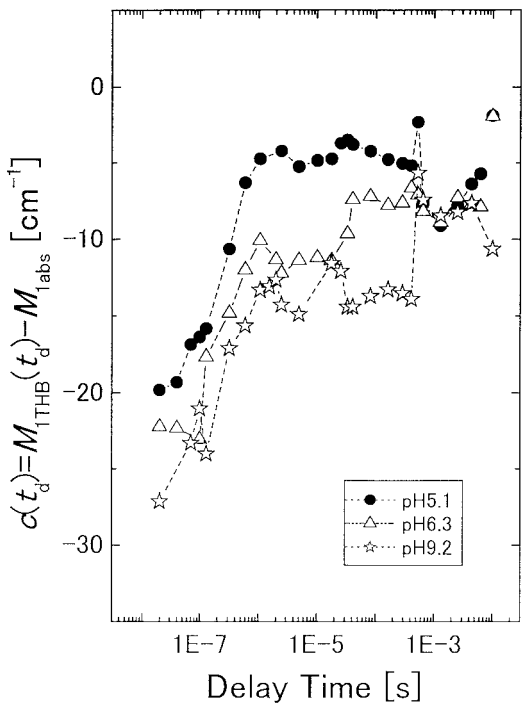

FIGURE 7 Time evolution of $c(t_d)$ for Zn-hsMb in aqueous solution at pH 5.1 (●), at pH 6.3 (△), and at pH 9.2 (☆). The data points are linked to each other by dashed lines to guides the eye.

DISCUSSION

Although the tertiary structure of Zn-Mb has not been determined yet, there have been a few experimental results providing information about the structural properties of Zn-Mb. Our previous measurement of the circular dichroism spectrum of Zn-Mb has shown that the Zn substitution results in no drastic alteration in the secondary structure (Shibata et al., 1998). We have also shown that the tertiary structure of Zn-Mb is maintained after the Zn substitution from the observation of its rotational-relaxation process (Shibata, 1997). Furthermore, Raman-scattering data have clearly indicated a similar five-coordinate state of the Zn atom in Zn-Mb to that of the Fe atom in deoxy-Mb, despite a slightly weaker coordination of the proximal His for Zn-Mb (Feitelson and Spiro, 1986). Here, accordingly, we assume similar heme-pocket conformations between deoxy-Mb and Zn-Mb and proceed to the following discussion.

An x-ray diffraction study on mutants has shown that the mutation His64→Leu results in removal of a water molecule, which is hydrogen-bonded to the distal His in the native deoxy-Mb (Quillin et al., 1993). This water molecule

has been considered to partially contribute to determine the association rate of ligand molecules (Carver et al., 1990; Uchida et al., 1997). It is also inferred that the conformational inhomogeneity of residue 64 is largely reduced by this mutation. This is because the substituted Leu with aprotic characteristics assumes only one conformational state regardless of pH, whereas the intact His residue assumes two distinct conformations due to the different protonation states, and the population of these two states is pH dependent. The pH-dependent conformation of His64 of Mb has been observed clearly by Yang and Phillips (1996) in their x-ray diffraction study. This pH-dependent conformational change in His64 has been explained quantitatively in the case of MbCO (Müller et al., 1999). A recent atomic-resolution diffraction study has also shown that deoxy-Mb exhibits two different conformations of His64 with equal occupancies at neutral pH (Vojtěchovský et al., 1999). These two conformations may correspond to the low-pH and neutral-pH conformations observed by Yang and Phillips. These experimental results thus have given clear evidences for a loose characteristic of His64.

Whether the hydrogen-bonded water molecule moves with the distal His according to its conformational change is ambiguous at present. Yang and Phillips (1996) has modeled that the water molecule moves with the distal His upon its conformational change caused by the pH change. Vojtvěchovský et al. (1999), on the other hand, has put the water molecule at one position although they modeled the distal His to assume two distinct conformations. Thus, it is not clear in their model whether the water molecule moves with the His64 residue.

As shown in Figs. 3 and 5, the present study has revealed a drastic reduction of the inhomogeneous broadening and the amplitude of the temporal shift of the THB spectrum upon the mutation of His64→Leu. The native sample shows a broader and rather asymmetric Q-band absorption profile, whereas the H64L-mutant sample shows a much sharper one with almost complete symmetry. These results suggest that in the H64L mutant the conformational disorder around the position-64 residue is substantially suppressed. This leads us to infer a strong relation between the observed process in the TRTHB experiment and the motion around the distal histidine in the case of the native samples. On the other hand, we can say here that the contribution of the motion of the proximal side to the observed process is, even if it exists, very small, despite the strong interaction through the direct covalent bond. This is consistent with the analysis of Vojtěchovský et al. (1999) suggesting a more rigid character of the proximal side. Their analysis of anisotropic disorder of atoms has suggested that the proximal F helix can be well described by a single rigid-body group, contrary to the case of the more flexible E helix.

The interconversion of His64 between the two distinct conformations observed by the above described x-ray diffraction studies seems to be a plausible candidate for the origin of the inhomogeneous broadening and the temporal shift of the THB spectrum of the Zn-Mb sample. This interpretation seems also consistent with the pH-dependent shift of the absorption spectrum of Zn-Mb taking place in the pH region between 5 and 7. As observed by Müller et al. (1999), in the pH region between 5 and 7, both the protonated and the unprotonated states of His64 and His97 coexist, and the population of each state depends on pH. Therefore, in this pH region, the change in the population of the protonation states of His64, and possibly together with that of His97, may cause the shift of the absorption spectrum with varying pH. Above pH 7, the unprotonated state of both histidine residues dominates, and then the absorption spectrum becomes no longer sensitive to pH.

The above interpretation seems to be successful in giving a qualitative explanation of the present results. However, a more careful inspection of the data reveals that the above interpretation does not explain well the experimental results on a quantitative level. If the interconversion of His64 between its protonation states is the main source of the inhomogeneous broadening, the width of the absorption spectrum is expected to significantly broaden more in the pH region 5–7 than outside this pH region due to the coexistence of distinct protonation states of His64. As shown in Fig. 2 *b*, however, the increase of σ_{abs} upon lowering pH from 8 to 6 is only a few cm^{-1}, that is much smaller as compared with the $\sim$30-cm^{-1} shift of the absorption upon the same pH change. Thus, only a slight broadening of the absorption width upon a pH change from 8 to 6 suggests that although the conformational interconversion of His64 indeed has an influence on the absorption spectrum, it has only a minor contribution to broaden the absorption width. The above interpretation also leads to an expectation that the temporal shift of the THB spectrum is largely reduced at a high pH of 9 where the unprotonated state of His64 dominates. This again contradicts to the experimental results as shown in Fig. 7. Accordingly, we suppose here that the absorption shift with varying pH is dominantly induced by a continuous alteration of the conformation around Zn-PP upon pH change, which partly results from the protonation-state change in His64 and His97.

As discussed above, here we conclude that the conformational disorder of His64 is only the minor source of the inhomogeneous broadening of Zn-Mb. Here, we tentatively propose an alternative postulate that the positional and rotational fluctuations of the water molecule hydrogen-bonded to the distal His is the main origin of the inhomogeneous broadening. A large dipole moment of a water molecule implies that its rotational fluctuation is likely to have a strong influence on the electronic state of Zn-PP. It is also possible that in the distal pocket there exist several water molecules other than that attached to His64, although they are not observed in the x-ray diffraction studies due to the disorder. Such sequestered water molecules would

seem, if they actually exist, likely to have a substantial contribution to the inhomogeneous broadening. This explanation is consistent with the two important findings of the present experiment: 1) that a largely reduced inhomogeneous broadening is observed for the H64L mutant in which the water molecule attached to the residue 64 is excluded and 2) that there is no evident pH dependence of the inhomogeneous broadening and of the temporal behavior of the THB spectrum for the native samples. This water molecule remains in the pocket regardless of the protonation state of the distal His, and then the present interpretation is consistent with the second experimental finding. This water molecule is known to play an important role in determining the association rate of a ligand molecule (Carver et al., 1990; Quillin et al., 1993; Uchida et al., 1997). It has also been suggested to contribute crucially to preserve the conformational flexibility of Mb (Sastry and Agmon, 1997). Hence, the motion of this water molecule within the heme pocket has a crucial importance in the function of Mb.

The amplitude of the temporal shift of $c(t_d)$ at 240 K amounts to $\sim$60 cm^{-1} and 20 cm^{-1} for the native and the H64L-mutant sample, respectively. With an assumption that the 20-cm^{-1} shift of the THB spectrum for the H64L-mutant sample comes purely from the motion of the protein matrix, the residual $\sim$40-cm^{-1} shift for the native sample is expected to be induced by the motion of the water. By assuming the dipole-dipole interaction between the chromophore and the water molecule, we can evaluate the shift of the transition energy $\Delta\nu$ induced by the rotation of the water molecule in the distal pocket as

$$\Delta\nu \sim \left| -\frac{\mu_{H_2O}\Delta\mu}{2\pi\epsilon hc} \times \frac{1}{R^3} \right|. \quad (6)$$

Here, ϵ is the permittivity in vacuum, h is Planck's constant, c is the velocity of light, μ_{H_2O} is the dipole moment of a water molecule, $\Delta\mu$ is the difference of the static dipole moment between the excited and ground state of the chromophore, and R is the water-chromophore distance. $\Delta\mu$ of Zn-PP in Mb has been evaluated to be on the order of 0.5 D from the Stark-effect study of the absorption spectrum (unpublished result). The dipole moment of a water molecule is $\sim$2 D, and the water-chromophore distance is estimated to be $\sim$3.5 Å (Vojtěchovský et al., 1999). Putting these values into Eq. 6, $\Delta\nu$ is estimated to be $\sim$19 cm^{-1}. This value is roughly on the same order as that of 40-cm^{-1} shift of the THB spectrum attributed to the water motion. A part of the deviation is possibly due to the invalidity of the dipole-dipole interaction between very closely located molecules, which may interact more strongly than the dipole-dipole coupling.

There is a somewhat unusual aspect in the present interpretation of the water-motion-induced inhomogeneous broadening. If this interpretation is true, the previously observed strong correlation between solvent viscosity and the time scale of the temporal variation of the THB spectrum (Shibata et al., 1999) requires a strong coupling between solvent viscosity and the motion of the internal water within the distal pocket. Investigations of the solvent effect on the ligand-rebinding kinetics of Mb have shown, on the other hand, that the geminate-rebinding kinetics, which is an internal process within the protein matrix, is almost independent of viscosity, whereas the bimolecular process is highly viscosity dependent (Beece et al., 1980; Kleinert et al., 1998). As compared with this observation, it is an unusual point of the present interpretation that a completely internal process of the water motion within the pocket is strongly coupled with solvent viscosity. This can be explained by assuming that such fluctuations of the internal water are coupled with the global conformational fluctuation of protein, which is viscosity dependent.

Barboy and Feitelson (1987, 1989) have estimated the diffusion rate of various molecules through the Zn-Mb matrix from the measurement of the quenching rate of the triplet state of Zn-porphyrin by these molecules. From the analysis of the temperature dependence of the diffusion rate, they have estimated the activation energy of the diffusion through the protein matrix. Their analysis has shown that the activation energies are almost same for the different molecules within the experimental error, despite different molecular sizes. They have concluded from this observation that the rate-limiting step of the diffusion of a small molecule through the Mb matrix is the conformational change that opens the pathway for the diffusion. Their conclusion is quite compatible with our interpretation drawn here. It is likely that the water molecule can migrate within the distal pocket only when steric hindrances are removed by the conformational fluctuation of the protein matrix. In this case, the water molecule can be regarded as a sensitizer of the conformational fluctuation of the protein matrix. Possibly, involvement of the entrance and exit processes of the water molecule in the observed dynamics may also contribute to the observed strong coupling between solvent viscosity and the fluctuation time scale.

The conclusions drawn here rely crucially on the assumption of similar structure and dynamics of Mb in a solution phase and in a crystalline phase. This problem has been debated for a long time (Šrajer et al., 1996; Nienhaus et al., 1998). We should always consider the possibility that the fluctuation dynamics of a protein in an aqueous solution is significantly different from that in a crystal. The lack of the crystal-structure determination of Zn-Mb is also a serious deficiency of the present analysis. From these viewpoints, determination of the crystal structure of Zn-Mb and comparison of the fluctuation dynamics between a solution sample and a crystal sample is an important future problem. Furthermore, systematic investigations of the TRTHB method on various mutants are also an important future problem, which will help to validate the present conclusion.

REFERENCES

Ahn, J. S., T. Kitagawa, Y. Kanematsu, Y. Nishikawa, and T. Kushida. 1995. Glass transition of Zn-substituted myoglobin probed by absorption and site-selective fluorescence spectroscopies. *J. Luminesc.* 64:81–86.

Alben, J. O., D. Beece, S. F. Bowne, W. Doster, L. Eisenstein, H. Frauenfelder, D. Good, J. D. McDonald, M. C. Marden, P. P. Moh, L. Reinisch, A. H. Reynolds, E. Shyamsunder, and K. T. Yue. 1982. Infrared spectroscopy of photodissociated carboxymyoglobin at low temperatures. *Proc. Natl. Acad. Sci. U.S.A.* 79:3744–3748.

Ansari, A., J. Berendzen, S. F. Bowne, H. Frauenfelder, I. E. T. Iben, T. B. Sauke, E. Shyamsunder, and R. D. Young. 1985. Protein states and proteinquakes. *Proc. Natl. Acad. Sci. U.S.A.* 82:5000–5004.

Austin, R. H., K. W. Beeson, L. Eisenstein, H. Frauenfelder, and I. C. Gunsalus. 1975. Dynamics of ligand binding to myoglobin. *Biochemistry.* 14:5355–5373.

Barboy, N., and J. Feitelson. 1987. Quenching of the zinc-protoporphyrin triplet state as a measure of small molecule diffusion through the structure of myoglobin: environmental effects. *Biochemistry.* 26: 3240–3244.

Barboy, N., and J. Feitelson. 1989. Diffusion of small molecules through the structure of myoglobin: environmental effects. *Biochemistry.* 28: 5450–5456.

Beece, D., L. Eisenstein, H. Frauenfelder, D. Good, M. C. Marden, L. Reinisch, A. H. Reynolds, L. B. Sorensen, and K. T. Yue. 1980. Solvent viscosity and protein dynamics. *Biochemistry.* 19:5147–5157.

Carlson, M. L., R. M. Regan, and Q. H. Gibson. 1996. Distal cavity fluctuations in myoglobin: protein motion and ligand diffusion. *Biochemistry.* 35:1125–1136.

Carver, T. E., R. S. Rohlfs, J. S. Olson, Q. H. Gibson, R. S. Blackmore, B. A. Springer, and S. G. Sligar. 1990. Analysis of the kinetic barriers for ligand binding to sperm whale myoglobin using site-directed mutagenesis and laser photolysis techniques. *J. Biol. Chem.* 265: 20007–20020.

Elber, R., and M. Karplus. 1990. Enhanced sampling in molecular dynamics: use of the time-dependent Hartree approximation for a simulation of carbon monoxide diffusion through myoglobin. *J. Am. Chem. Soc.* 112:9161–9175.

Feitelson, J., and T. G. Spiro. 1986. Bonding in zinc proto- and mesoporphyrin substituted myoglobin and model compounds studied by resonance Raman spectroscopy. *Inorg. Chem.* 25:861–865.

Frauenfelder, H., G. A. Petsko, and D. Tsernoglou. 1979. Temperature-dependent x-ray diffraction as a probe of protein structural dynamics. *Nature.* 280:558–563.

Frauenfelder, H., S. G. Sligar, and P. G. Wolynes. 1991. The energy landscapes and motions of proteins. *Science.* 254:1598–1603.

Jackson, T. A., M. Lim, and P. A. Anfinrud. 1994. Complex nonexponential relaxation in myoglobin after photodissociation of MbCO: measurement and analysis from 2 ps to 56 μs. *Chem. Phys.* 180:131–140.

Kinoshita, S. 1989. Theory of transient hole-burning spectrum for molecules in solution. *J. Chem. Phys.* 91:5175–5184.

Kleinert, T., W. Doster, H. Leyser, W. Petry, V. Schwarz, and M. Settles. 1998. Solvent composition and viscosity effects on the kinetics of CO binding to horse myoglobin. *Biochemistry.* 37:717–733.

Kurita, A., Y. Kanematsu, and T. Kushida. 1990. Non-photochemical hole-burning in Zn-substituted myoglobin. *J. Luminesc.* 45:317–319.

Müller, J. D., B. H. McMahon, E. Y. T. Chien, S. G. Sligar, and G. U. Nienhaus. 1999. Connection between the taxonomic substates and protonation of histidine 64 and 97 in carbonmonoxy myoglobin. *Biophys. J.* 77:1036–1051.

Nienhaus, G. U., K. Chu, and K. Jesse. 1998. Structural hetrogeneity and ligand binding in carbonmonoxy myoglobin crystals at cryogenic temperatures. *Biochemistry.* 37:6819–6823.

Quillin, M. L., R. M. Arduini, J. S. Olson, and G. N. Phillips, Jr. 1993. High-resolution crystal structure of distal histidine mutants of sperm whale myoglobin. *J. Mol. Biol.* 234:140–155.

Sastry, G. M., and N. Agmon. 1997. Trehalose prevents myoglobin collapse and preserves its internal mobility. *Biochemistry.* 36:7097–7108.

Shibata, Y. 1997. Studies of conformational dynamics of myoglobin by time-resolved hole-burning spectroscopy. Ph.D. thesis. Osaka University, Osaka, Japan.

Shibata, Y., A. Kurita, and T. Kushida. 1996. Transient hole-burning spectroscopy of Zn-substituted myoglobin. *J. Luminesc.* 66&67:13–18.

Shibata, Y., A. Kurita, and T. Kushida. 1997. Temperature and solvent viscosity dependence of conformational dynamics of Zn-substituted myoglobin observed by nanosecond time-resolved transient hole-burning spectroscopy. *J. Luminesc.*72–74:605–606.

Shibata, Y., A. Kurita, and T. Kushida. 1998. Real-time observation of conformational fluctuation in Zn-substituted myoglobin by time-resolved transient hole-burning spectroscopy. *Biophys. J.* 75:521–527.

Shibata, Y., A. Kurita, and T. Kushida. 1999. Solvent effects on conformational dynamics of Zn-substituted myoglobin observed by time-resolved hole-burning spectroscopy. *Biochemistry.* 38:1789–1801.

Shibata, Y., and T. Kushida. 1998. Determination of Q_x- and Q_y- absorption bands of Zn-PP derivatives contained in proteins by hole-burning spectroscopy. *Chem. Phys. Lett.* 284:115–120.

Šrajer, V., T. Teng, T. Ursby, C. Pradervand, Z. Ren, S. Adachi, W. Schildkamp, D. Bourgeois, M. Wulff, and K. Moffat. 1996. Photolysis of the carbon monoxide complex of myoglobin: nanosecond time-resolved crystallography. *Science.* 274:1726–1729.

Tian, W. D., J. T. Sage, P. M. Champion, E. Chien, and S. G. Sligar. 1996. Probing heme protein conformational equilibration rates with kinetic selection. *Biochemistry.* 35:3487–3502.

Uchida, T., K. Ishimori, and I. Morishima. 1997. The effect of heme pocket hydrophobicity on the ligand binding dynamics in myoglobin as studied with leucine 29 mutants. *J. Biol. Chem.* 272:30108–30114.

Varadarajan, R., A. Szabo, and S. G. Boxer. 1985. Cloning expression in *Escherichia coli* and reconstruction of human myoglobin. *Proc. Natl. Acad. Sci. U.S.A.* 82:5681–5684.

Vojtěchovský, J., K. Chu, J. Berendzen, R. M. Sweet, and I. Schlichting. 1999. Crystal structures of myoglobin-ligand complexes at near-atomic resolution. *Biophys. J.* 77:2153–2174.

Yang, F., and G. N. Phillips, Jr. 1996. Crystal structures of CO-, deoxy- and met-myoglobins at various pH values. *J. Mol. Biol.* 256:762–774.

Young, R. D., H. Frauenfelder, J. B. Johnson, D. C. Lamb, G. U. Nienhaus, R. Philipp, and R. Scholl. 1991. Time- and temperature-dependence of large-scale conformational transitions in myoglobin. *Chem. Phys.* 158: 315–327.